ERURJ, 2023, 2, 4, 575-594

(Article)

Sliding-Mode Control of Horizontal Coupled-Tank Systems Using Variable-Speed Pump

Magdy R. Roman [1, *], Mina A. Louis [1], Osama M. Khorais [1]

[1] *Mechatronics and Robotics Engineering Department, Faculty of Engineering, Egyptian Russian University, 11829 Badr City, Cairo, Egypt.*

*Corresponding author(s): Magdy R. Roman, E-mail: magdy-raouf@eru.edu.eg

Received 9th July 2023, Revised 21th October 2023, Accepted 29th October 2023

DOI: 10.21608/ERURJ.2023.221947.1054

ABSTRACT

In many chemical and food processing industries, liquid is pumped into and held in interconnected linked tanks. Nevertheless, due to the high non-linearity and complexity of that system, level and flow regulation among these tanks is a non-trivial task. The current research focuses on the regulation of the liquid level in two horizontally linked tanks. The three most common sliding-mode control (SMC) algorithms that can be found in the literature—proportional-derivative SMC (PD-SMC), proportional-integral-derivative SMC (PID-SMC), and dynamic SMC—are compared. The impact of sensor noise on the functioning of the controller and the chattering phenomenon is highlighted in particular. Simulations are done for the proposed control algorithms. Using the MATLAB optimization toolbox, control parameters are chosen to improve the designed performance indices. Experiments are carried out on a designed test setup to investigate the effect of sensor noise. Results showed that PD-SMC has a superior performance over the other two algorithms, PID-SMC and dynamic-SMC both in simulation and experimental results.

Keywords: Horizontal coupled-tank, SMC, Dynamic-SMC, variable-speed control pump

1. Introduction

Several industrial sectors, including petrochemicals, drugs, and paper industries, utilize liquid-level control in multi-tank systems. However, because of its complexity and strong nonlinearity, a connected tank system poses a challenging control problem. To maintain a target liquid level irrespective of system uncertainty and external disturbances, an accurate model and an effective control strategy are crucial. Because of the PID controller's simple structure, many tuning techniques of its parameters have been adopted, [1], [2]. However, typical PID controller tuning methods fail to provide convenient behavior to coupled-tank systems. Furthermore, most PID algorithms were developed utilizing lower-order linearized process models [3-6]. The lower-order linearization causes further parametric uncertainty. There have been rare attempts to build higher-order models of PID controllers, [7], [8]. Moreover, a robustness measure should be considered throughout the design process in order to avoid model-uncertainty-caused problems. A comparison was carried out between PID and fuzzy control in [9]. For the nonlinear quadruple tank system, a controller based on Artificial Neural Network (ANN) was developed in [10]. Adaptive and backstepping algorithms were also applied in the coupled tank system [11-13]. Backstepping control based on observers, lag controller, and MPC are proposed in [14], [15], and [16] respectively. In [17], a robust nonlinear approach for the control of liquid levels in a quadruple tank system (QTS) is developed based on the design of an integrator backstepping super-twisting controller. Decentralized algorithms were designed to regulate the coupled tank system level [18] and [19]. In [20] and [21], a fractional-order proportional integral (FOPI) control for coupled tank systems was built. Integral-order PD (IOPD), integer-order PI (IOPI), cascaded FOPD, and FOPI control algorithms for the coupled tank system were compared in [22]. For nonlinear process control, fractional and integral order controllers were assessed and compared based on various models [23]. For managing the level of liquid in spherical connected tanks, a fuzzy FOPID algorithm was proposed in [24]. To address the level control in a multi-input multi-output coupled tank system, a FOID controller was devised [25]. Moreover, TS (Takage-Sugeno) fuzzy controller and fuzzy knowledge-based decoupled control are proposed in [26] and [27] respectively.

SMC offers various appealing characteristics, including good disturbance rejection, improved transient performance, and faster response. SMC laws are fundamentally more robust in case of uncertainties [28], [29]. The design and analysis of variable structure systems (VSS) with sliding modes were investigated in [30] and [31]. A fuzzy SMC with a nonlinear sliding surface was presented in [32], with a fuzzy logic controller utilized to improve the chattering phenomenon. An adaptive fuzzy SMC was presented in [33]. For better smoothness of the switching signal in the coupled tanks system, a neuro-fuzzy-SMC with a nonlinear sliding surface was designed [34]. Two controllers, backstepping PI-SMC, and PI-SMC were investigated for a quadruple tank in [35]. A SMC of static type for the coupled tanks problem was developed in [36]. Two distinct dynamic SMC algorithms were also developed to eliminate the chattering problem [36]. Feedback linearization in conjunction with the SMC algorithm was used in a quadruple tank system [37]. A SMC of the second order was developed in [38] and [39]. An observer-based control for a four-connected tank system employing higher-order SMC was presented in [40]. To minimize the disturbance effect on the connected tank system, an adaptive feed-forward second-order SMC was proposed [41]. A chattering-free SMC was developed in [42]. To enhance the tracking behavior of connected tanks under varied uncertainty, an SMC with a variable boundary layer was investigated in [43]. Fuzzy FOSMC was offered as a robust, chatter-free technique for connected tanks [44]. SMC was proposed for the MIMO quadruple tank with time delay compensation in [45].

Sensor signals suffer from noise in industrial settings. This could be due to a variety of factors, for example, lengthy connection of cables, vicinity to different electrical equipment, etc. The controller's ability to control these noises is significant in such instances. Numerous studies claimed that the SMC model is a robust fast controller capable of dealing with uncertain nonlinear systems. Nonetheless, the sensor noise effect on the chattering behavior of SMC hasn’t been addressed.

The current research conducted an examination to compare three controllers: PID-SMC, PD-SMC, and dynamic-SMC. Simulink-MATLAB was used to compare the performance of the three algorithms. The current research focuses in particular on the examination of the sensor noise effect on those SMC algorithm's behavior, specifically the chattering problem. The study is structured in six sections: Section 2 presents the concept of the connected tank. Section 3 proposes the design of the control algorithms. Section 4 discusses and displays the simulation results. Section 5 presents the experimental work and finally, Section 6 presents the conclusion.

2. Model of the coupled tank system

The governing equations for the horizontally connected tanks seen in Figure 1 are as follows:

$$C\frac{dh_1}{dt} = q - q_1, C\frac{dh_2}{dt} = q_1 - q_2, \tag{1}$$

where q is the inlet rate of flow (m^3/s), q_1 is the rate of flow between tanks 1 and 2 in (m^3/s), h_1 is the level of 1st tank in (m), h_2 is the level of 2nd tank (m), q_2 is a rate of flow out of 2nd tank in (m^3/s) and C is the cross-sectional area of 1st and 2nd tank in (m^2). The rates of flow q_1 and q_2 are expressed as follows,

$$q_1 = c_{12}\sqrt{2g(h_1 - h_2)} \quad \text{for } h_1 > h_2, \tag{2}$$

$$q_2 = c_2\sqrt{2gh_2} \quad \text{for } h_2 > 0, \tag{3}$$

where c_{12}, and c_2 are the coupling and outlet orifices areas (m^2), respectively, and g in (m^2/s) is the gravitational acceleration. The flow q into the 1st tank is positive in the connected tanks system since the pump only pumps water into the tank. Consequently, the inflow rate will be

$$q \geq 0 \tag{4}$$

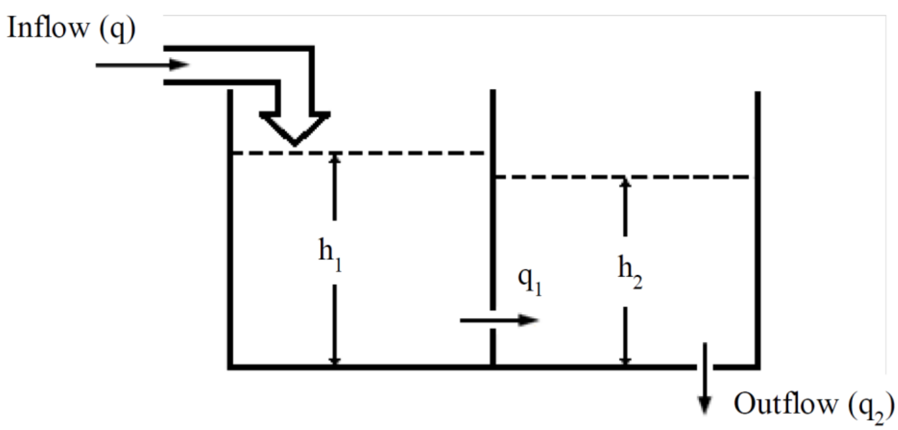

Figure 1. Horizontal connected tanks system

At equilibrium, the derivatives must be zero for a desired constant liquid level, i.e.,

$$\dot{h}_1 = \dot{h}_2 = 0, \tag{5}$$

therefore,

$$-\frac{c_{12}}{C}\sqrt{2g\,|h_1 - h_2|}\,\mathrm{sgn}(h_1 - h_2) + \frac{Q}{C} = 0, \frac{c_{12}}{C}\sqrt{2g\,|h_1 - h_2|}\,\mathrm{sgn}(h_1 - h_2) - \frac{c_2}{C}\sqrt{2gh_2} = 0 \tag{6}$$

where Q denotes the inflow rate at equilibrium. To justify the constraint applied to the inlet rate of flow in equation (4), $\mathrm{sgn}(h_1 - h_2)$ should be positive.

Considering $z_1 = h_2 > 0,\ z_2 = h_1 - h_2 > 0,\ \mathbf{Z} = \begin{bmatrix} z_1 \\ z_2 \end{bmatrix}$, u = q(t)

Also let $a_1 = \frac{c_2\sqrt{2g}}{c}$ & $a_2 = \frac{c_{12}\sqrt{2g}}{c}$

As a result, the dynamic model can be stated as

$$\dot{z}_1 = -a_1\sqrt{z_1} + a_2\sqrt{z_2}\ ,\dot{z}_2 = a_1\sqrt{z_1} - 2a_2\sqrt{z_2} + \frac{u}{c},\ y = z_1, \tag{7}$$

where $z_1 = h_2$ is regarded as the system output.

The objective of the control algorithm is to regulate the output $y(t) = z_1(t) = h_2(t)$ to the desired value h_{2d}. The dynamics of the coupled-tank system are nonlinear as can be observed. As a result, a transformation will be constructed in order to convert the model into another formula that will facilitate the design of the controller.

For the state $\boldsymbol{x} = \begin{bmatrix} x_1 \\ x_2 \end{bmatrix}$ we define a transformation $\boldsymbol{x} = T(\boldsymbol{z})$ as,

$$x_1 = z_1,\ x_2 = -a_1\sqrt{z_1} + a_2\sqrt{z_2} \tag{8}$$

The inverse transformation $\boldsymbol{z} = T^{-1}(\boldsymbol{x})$ is such

$$z_1 = x_1,\ z_2 = \left(\frac{a_1\sqrt{x_1} + x_2}{a_2}\right)^2 \tag{9}$$

The model in (7) is therefore expressed as,

$$\dot{x}_1 = x_2,\quad \dot{x}_2 = \frac{a_1 a_2}{2}\left(\frac{\sqrt{z_1}}{\sqrt{z_2}} - \frac{\sqrt{z_2}}{\sqrt{z_1}}\right) + \frac{a_1^2}{2} - a_2^2 + \frac{a_2}{2c}\frac{1}{\sqrt{z_2}}u \tag{10}$$

where z_1 and z_2 values are a function of x_1 and x_2 as indicated by (9).

Therefore, system dynamics is represented as,

$$\dot{x}_1 = x_2,\quad \dot{x}_2 = f + \phi u,\ y = x_1, \tag{11}$$

where,

$$f = \frac{a_1 a_2}{2}\left(\frac{\sqrt{z_1}}{\sqrt{z_2}} - \frac{\sqrt{z_2}}{\sqrt{z_1}}\right) + \frac{a_1^2}{2} - a_2^2,\ \phi = \frac{a_2}{2c}\frac{1}{\sqrt{z_2}} \tag{12}$$

3. Controller design

SMC is a type of control algorithm that is robust and nonlinear and based on the Lyapunov method. In this method, an n^{th} order uncertain and nonlinear system is transformed into a 1^{st} order system. The numerous advantages of SMC include its very straightforward design and durability in handling dynamic characteristics and environmental disturbances. It is generally acknowledged that SMC offers a reliable solution to the control problem; as a result, it enables adapting to changes in the plant without noticeably diminishing the performance. Although SMC yields discontinuity in control results, it is obvious that the proposed control must direct the trajectory towards the switching surface and then be preserved on this surface. While using the SMC control algorithm, a problem encountered is to make the system respond to follow a particular trajectory.

The following single input single output system will be used to introduce the technique [28]:

$$x^{(n)} = f(x) + \phi(x).u, \tag{13}$$

where f and ϕ are nonlinear functions of the states, u is the input, and x is the vector of states of order n. The control's goal is that the state should remain bound to the vector state trajectory $x_d(t)$. Taking into account the surface S(t):

$$S(x,t) = \left(\frac{d}{dt} + \lambda\right)^{n-1} \tilde{x} \tag{14}$$

where $\tilde{x} = x - x_d$ denotes the error and λ is a constant > 0. Taking into consideration $V = 0.5S^2$ as a Lyapunov function, the control law must minimize the distance to the surface in (14) as well as all system states trajectory (slide mode). This is to say,

$$0.5\frac{d}{dt}S^2 \leq -\eta|S|, \tag{15}$$

where the constant η is > 0. The entire state trajectory was plainly improved, becoming closer to the sliding surface in finite time, and will remain there indefinitely. It is argued that the sliding mode($\dot{S} = 0$) occurred when the system is settled upon the surface.

As the surface is entered for the first time, the time is,

$$t_{reach} \leq \frac{S(0)}{\eta} \tag{16}$$

Using SMC, during its ideal two phases; reaching and sliding, the motion is restricted to the sliding surface [28]. The design process of the sliding mode has two steps. Firstly, designing a switching function S = 0 ensures that the sliding motion fulfills design requirements. Secondly, considering how the control law that will be chosen would describe the sliding mode in order to ensure that the conditions of presence and reaching are met [46]. The three different approaches for designing switching surfaces for a connected tank are described in the following subsections.

3.1 Sliding surface with PD control

Given that H is the reference signal, the system error can be defined as

$$e = (h_2 - H) = (z_1 - H) \tag{17}$$

Then, PD-SMC will be

$$S = K_p e + K_d \dot{e} = K_p(z_1 - H) + K_d \dot{z}_1 \tag{18}$$

Differentiating (18) in terms of time, yields

$$\dot{S} = K_d \ddot{z}_1 + K_p \dot{z}_1 \tag{19}$$

$$\dot{S} = K_d\left((-a_1 \dot{z}_1/2\sqrt{z_1}) + (a_2 \dot{z}_2/2\sqrt{z_2})\right) + K_p \dot{z}_1 \tag{20}$$

Solving (7) and (20) gives

$$\dot{S} = K_d\left[\frac{a_1^2 - 2a_2^2}{2} + \left(\frac{a_1 a_2}{2}\right)\left(\frac{\sqrt{z_1}}{\sqrt{z_2}} - \frac{\sqrt{z_2}}{\sqrt{z_1}}\right) + \left(\frac{a_2}{2C\sqrt{z_2}}\right)u\right] + K_p(-a_1\sqrt{z_1} + a_2\sqrt{z_2}) \tag{21}$$

In order to verify the Lyapunov criterion, it is assumed that

$$\dot{S} = -K\,\mathrm{sgn}(S) \tag{22}$$

where $\mathrm{sgn}(S) = \begin{cases} +1, & \text{if } S > 0, \\ 0, & \text{if } S = 0, \\ -1, & \text{if } S < 0, \end{cases}$

substituting in (21)

$$-K\,\mathrm{sgn}(S) = K_d\left[\frac{a_1^2 - 2a_2^2}{2} + \left(\frac{a_1 a_2}{2}\right)\left(\frac{\sqrt{z_1}}{\sqrt{z_2}} - \frac{\sqrt{z_2}}{\sqrt{z_1}}\right) + \left(\frac{a_2}{2C\sqrt{z_2}}\right)u\right] + K_p(-a_1\sqrt{z_1} + a_2\sqrt{z_2}) \tag{23}$$

gives,

$$u = \left(\frac{2C\sqrt{z_2}}{a_2}\right)\left[-\frac{a_1^2}{2} + a_2^2 - \left(\frac{a_1 a_2}{2}\right)\left(\frac{\sqrt{z_1}}{\sqrt{z_2}} - \frac{\sqrt{z_2}}{\sqrt{z_1}}\right)\right] - (K_p K_d)(-a_1\sqrt{z_1} + a_2\sqrt{z_2}) - (K/K_d)\,\mathrm{sgn}(S) \tag{24}$$

The system states are now approaching the hyperplane using the control law in the equation above. The error vectors are compelled to tend to zero. Concurrently, the height $h_2(t)$ will converge to the required value H. The SMC ensures that the output will asymptotically converge to the desired value.

The chattering problem affects the switching function. The chattering is caused by the sign function in the control signal. This implies that the control may change the value at any time without delay. Using the saturation function [28] could minimize chattering.

$$K\,\mathrm{sat}\left(\frac{S}{\Delta}\right) = \begin{cases} +1 & \text{for } (S/\Delta) \geq 1 \\ S/\Delta & \text{for } -1 < S < 1 \\ -1 & \text{for } (S/\Delta) \leq 1 \end{cases} \tag{25}$$

where K > 0 is the switching gain and Δ is the width of the boundary layer.

Using the saturation function to rewrite equation (24), gives,

$$u=\left(\frac{2C\sqrt{z_2}}{a_2}\right)\left[-\frac{a_1^2}{2}+a_2^2-\left(\frac{a_1a_2}{2}\right)\left(\frac{\sqrt{z_1}}{\sqrt{z_2}}-\frac{\sqrt{z_2}}{\sqrt{z_1}}\right)-\frac{(K_p}{K_d}\right)(-a_1\sqrt{z_1}+a_2\sqrt{z_2})-\left(\frac{K}{K_d}\right)\mathrm{sat}\left(\frac{S}{\Delta}\right) \quad (26)$$

3.2 Sliding surface with PID control

The PID model assists in quickly bringing the output of the system to the designed value ensuring minimal error and overshoot [47]. Because of its low cost and simplicity, it is the widely used controller in the industry.

The PID-SMC is constructed as:

$$S=K_pe+K_I\int e\,dt+K_d\dot{e}=K_p(z_1-H)+K_I\int(z_1-H)dt+K_d\dot{z}_1 \quad (27)$$

Differentiating (27) in terms of time leads to

$$\dot{S}=K_p\dot{z}_1+K_I(z_1-H)+K_d\ddot{z}_1 \quad (28)$$

Solving (7) and (28), gives

$$\dot{S}=K_p(a_2\sqrt{z_2}-a_1\sqrt{z_1})+K_I(z_1-H)+K_d[\frac{a_1^2-2a_2^2}{2}+\left(\frac{a_1a_2}{2}\right)\left(\frac{\sqrt{z_1}}{\sqrt{z_2}}-\frac{\sqrt{z_2}}{\sqrt{z_1}}\right)+\left(\frac{a_2}{2C\sqrt{z_2}}\right)u] \quad (29)$$

Providing a procedure same as introduced in (24), for $\dot{S}$ to be zero,

$$u=\left(\frac{2C\sqrt{z_2}}{a_2}\right)\left[-\left(\frac{K_P}{K_d}\right)(a_2\sqrt{z_2}-a_1\sqrt{z_1})-\left(\frac{K_I}{K_d}\right)(z_1-H)-\frac{a_1^2}{2}+a_2^2-\left(\frac{a_1a_2}{2}\right)\left(\frac{\sqrt{z_1}}{\sqrt{z_2}}-\frac{\sqrt{z_2}}{\sqrt{z_1}}\right)\right]-\left(\frac{K}{K_d}\right)\mathrm{sat}\left(\frac{S}{\Delta}\right) \quad (30)$$

3.3 Dynamic sliding mode controller

A dynamic SMC is introduced [36] to reduce chattering caused by static-SMC (PD-SMC). Assuming the scalers α_1, α_2 are positive, then sliding surface S is defined as follows,

$$S=\ddot{x}_1+\alpha_1\dot{x}_1+\alpha_2(z_1-H) \quad (31)$$

where x_1 is defined (11) and (12).

Sub. (11) and (12) in (31) gives,

$$S=\left(\frac{a_1a_2}{2}\right)\left(\frac{\sqrt{z_1}}{\sqrt{z_2}}-\frac{\sqrt{z_2}}{\sqrt{z_1}}\right)+\frac{a_1^2}{2}-a_2^2+\frac{a_2}{2C}\frac{1}{\sqrt{z_2}}u+\alpha_1(-a_1\sqrt{z_1}+a_2\sqrt{z_2})+\alpha_2(z_1-H) \quad (32)$$

Differentiating equation (31) in terms of time, and substituting from (8) and (10),

$$\begin{aligned}\dot{S}&=\dddot{x}_1+\alpha_1\ddot{x}_1+\alpha_2\dot{x}_1\\&=f_1+\alpha_1\left(\frac{a_1a_2}{2}\left(\frac{\sqrt{z_1}}{\sqrt{z_2}}-\frac{\sqrt{z_2}}{\sqrt{z_1}}\right)+\frac{a_1^2}{2}-a_2^2+\frac{a_2}{2C}\frac{1}{\sqrt{z_2}}u\right)+\alpha_2(a_2\sqrt{z_2}-a_1\sqrt{z_1})+\frac{a_2}{2C}\frac{1}{\sqrt{z_2}}\dot{u}-\\&\quad\frac{a_2}{4C}\frac{1}{\sqrt{z_2^3}}\left(a_1\sqrt{z_1}-2a_2\sqrt{z_2}+\frac{1}{C}u\right)u\end{aligned} \quad (33)$$

To meet the Lyapunov stability criterion, equation (33) is modified, where $\dot{S} = -K\mathrm{sat}(S/\Delta)$, as follows,

$$\dot{u} = \frac{-2C\sqrt{z_2}}{a_2}\left[f_1 + \alpha_1\left(\frac{a_1 a_2}{2}\left(\frac{\sqrt{z_1}}{\sqrt{z_2}} - \frac{\sqrt{z_2}}{\sqrt{z_1}}\right) + \frac{a_1^2}{2} - a_2^2 + \frac{a_2}{2C}\frac{1}{\sqrt{z_2}}u\right) + \alpha_2(-a_1\sqrt{z_1} + a_2\sqrt{z_2}) + K\mathrm{sat}\left(\frac{S}{\Delta}\right)\right] + \frac{1}{2z_2}\left(a_1\sqrt{z_1} - 2a_2\sqrt{z_2} + \frac{1}{C}u\right)u \tag{34}$$

where,

$$f_1 = \frac{-a_1 a_2(z_1+z_2)}{4\sqrt{(z_1 z_2)^3}} * \left(a_1 {z_1}^{\frac{3}{2}} - 2a_2 z_1\sqrt{z_2} + \frac{1}{C}z_1 u + a_1 z_2\sqrt{z_1} - a_2 {z_2}^{\frac{3}{2}}\right) \tag{35}$$

The state trajectories co-occurring with the discontinuous function in equation (22) reveal a finite-time accessibility to zero starting from random initial conditions providing that K > 0. Since S is forced to zero, the output y = z_1 = h_2 is regulated by the second-order dynamics $\ddot{y} + \alpha_1\dot{y} + \alpha_2(y - H) = 0$ after such a finite time as a result, because α_1 and α_2 are positive scalars, the output y(t) will converge asymptotically to the required value H.

4. Results of Simulation

There are four to five tuning parameters for each control algorithm. In this case, it is impractical to select controller parameters through trial and error, as has been done in many prior studies, to obtain specific response requirements. The optimization toolbox of MATLAB is utilized in this study to determine the controller parameters' optimum values. The toolbox offers many tools for minimizing or maximizing objectives and functions while meeting specific restrictions. In this research, the method of gradient descent optimization is applied for its simplicity and effectiveness. Figure 2 depicts the optimization constraints applied in the three algorithms. The rise time (based on 90% of the final value) is set to 35 seconds, settling time (based on ±5% of the final value) is set to 100 seconds, overshoot is set to 8%, and undershoot is set to 5%.

Two objective functions are chosen. The first one is the integral of the square of the difference in height between the level of liquid, h_2, and the required height, h_{2d}. This is referred to as the index of error and is given by,

$$Q_1 = \int (h_2 - h_{2d})^2 \, .dt \tag{36}$$

The integral of the square of the control signal time derivative, u, is the second objective function. This function will be referred to as the index of chattering and is defined as

$$Q_2 = \int \left(\frac{du}{dt}\right)^2 .dt \tag{37}$$

As the rate of chattering of the signal reduces, so does this index given by (37). By minimizing (36) and (37) and maintaining the signal within the limitations specified above, the controller's optimum performance is provided. The optimization algorithm seeks the optimal combinations of controller parameters to achieve this goal. Table 1 illustrates the controller parameters search range.

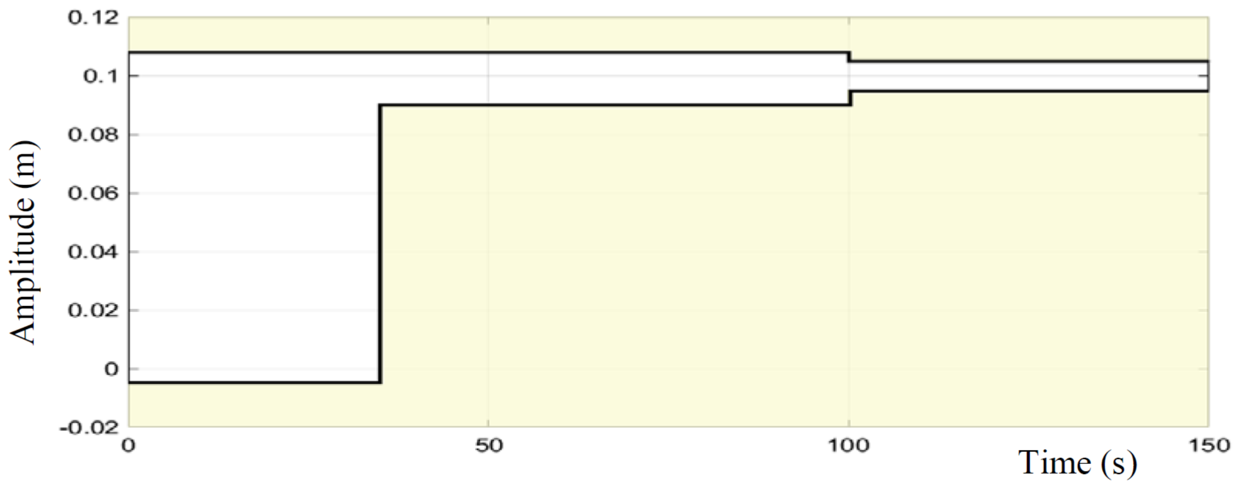

Figure 2. Signal constraints

Table 1. Controller parameters search range

Coefficient	Range	Coefficient	Range
K	zero→∞	α_1	zero →∞
Δ	zero →∞	α_2	zero →∞
K_p	zero →∞		
K_I	zero →∞		
K_d	zero →∞		

A 0.1-meter step input is applied to the connected tank system. Table 2 displays the parameters identified by the optimization technique for each controller to make the response meet the constraints indicated in Fig. 4 and fulfill both objective functions (36) and (37). Figures 3–5 depict the three control algorithms' responses to this disruption. Those figures show that PD-SMC, PID-SMC, and Dynamic-SMC have all met the desired level (steady-state error = 0) The PID-

SMC has a maximum overshoot of 4.9 percent, while the PD-SMC has the least overshoot of 1.59 percent. As observed in figures 3-b to 5-b, the three algorithms almost have no chattering. Table 3 compares the rising time, overshoot percentage, steady-state error, index of error, and settling time (five percent criterion) for the three controllers. According to the table, PD-SMC has the lowest index of error.

Table 2. Controllers tuning parameters

Parameter	PD-SMC	PID-SMC	Dynamic-SMC
K	2	10.2	1.036
Δ	0.832	47.213	0.406
K_p	8.55	1.828	-
K_I	-	$1.0*10^{-5}$	-
K_d	50.865	1.099	-
α_1	-	-	0.233
α_2	-	-	0.012

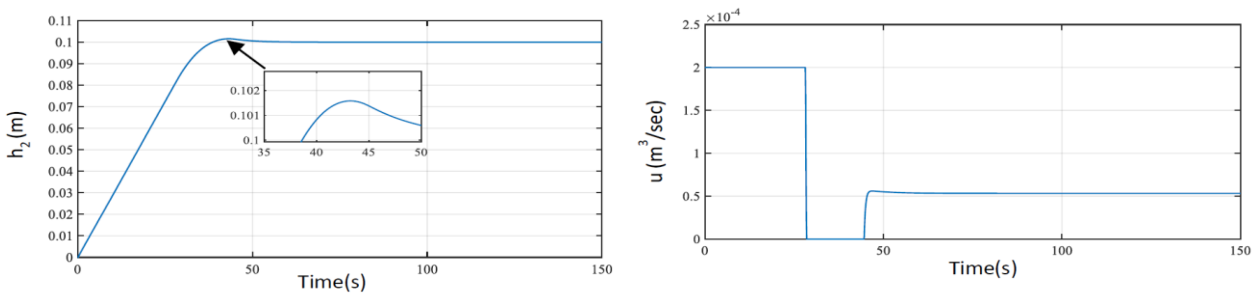

(A) (B)

Figure 3. Performance of PD-SMC (A) 0.1 m step response, (B) Control signal

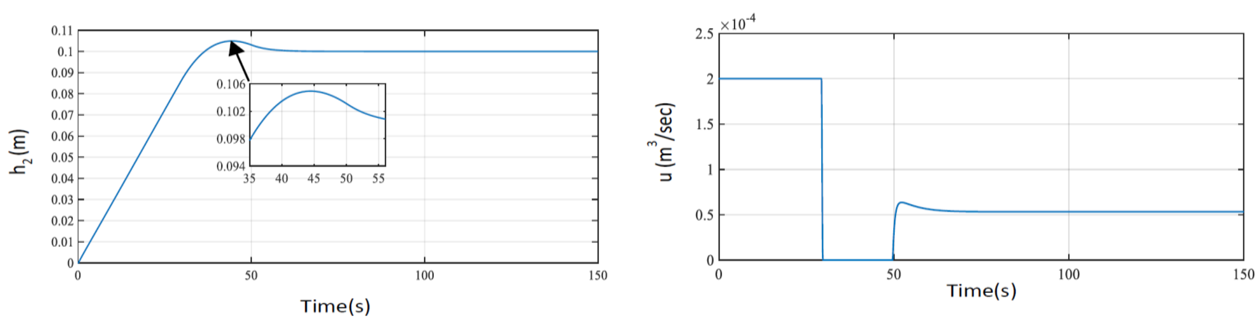

(A) (B)

Figure 4. Performance of PID-SMC (A) 0.1 m step response, (B) Control signal

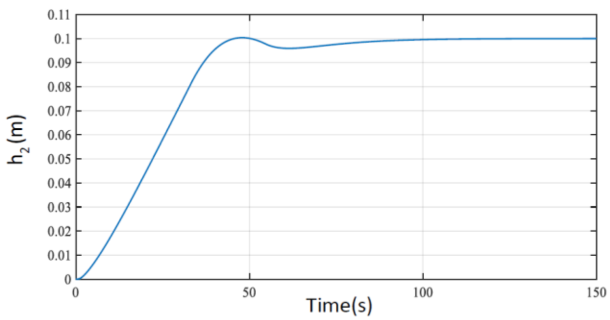

(A)

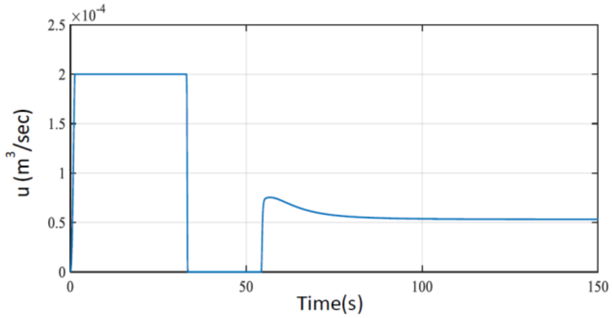

(B)

Figure 5. Performance of dynamic-SMC (A) 0.1 m step response, (B) Control signal

Table 3. Step response comparison for the three SMC algorithms

Algorithm	Rise time (s)	Overshoot (%)	Steady-state error (m)	Error index (m^2.s)	Settling time (s)
PD-SMC	29	1.59	0	0.116	34
PID-SMC	28	4.85	0	0.117	33.6
Dynamic-SMC	31	--	0	0.158	40

5. Experimental Results

5.1 System description

This section discusses the description of the experimental setup used to validate the mathematical model and test the performance of the developed control algorithm. The system shown in Fig. 6 consists of four water tanks, the dimensions of each tank are 15×15×35 cm^3, with a maximum capacity of 7.88 L. These tanks can be connected in different configurations to facilitate investigating different coupled tank problems. However, the system will be used here to investigate the horizontal coupled tank problem. The main water tank at the bottom feeds two separately operated variable speed centrifugal pumps to control the output flow rates. All connections are made by ½" copper pipes with 13 manually controlled ball valves.

Fig. 7 shows a schematic drawing of the main components used in controlling and monitoring the tank levels. The system consists of:

- Two calibrated level sensors (eTape – resistive type) with voltage divider circuit.

- A Variable Frequency Drive (VFD); frequency inverter (AC-220 V) connected with a PWM to an analogue converter circuit.
- Centrifugal pump (model QB – 60 with max. flow = 35 L/min and max. head = 35 m)
- Microcontroller (Arduino Mega 2560).
- Host computer for data monitoring and recording

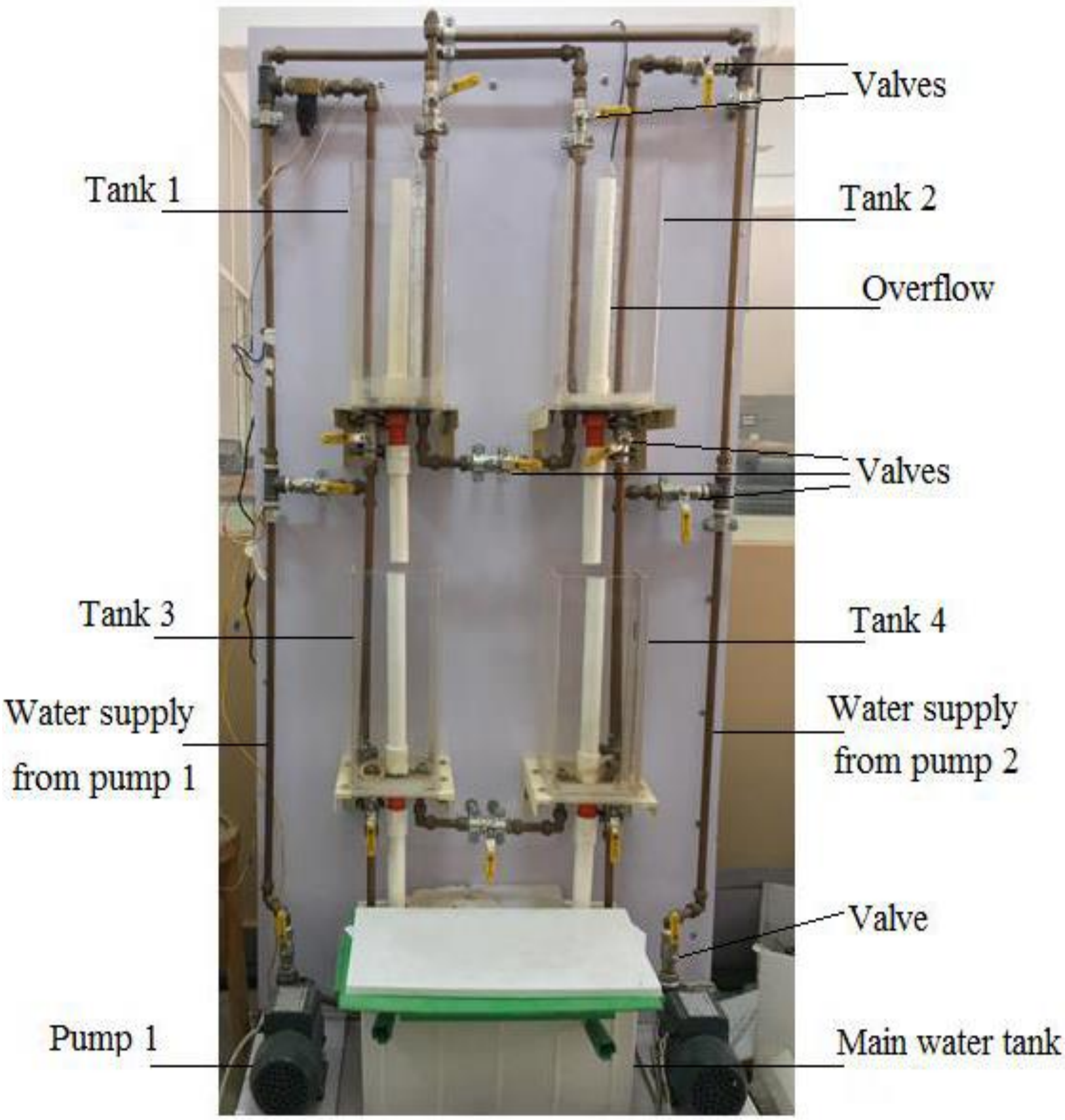

Figure 6. Coupled tanks liquid level system

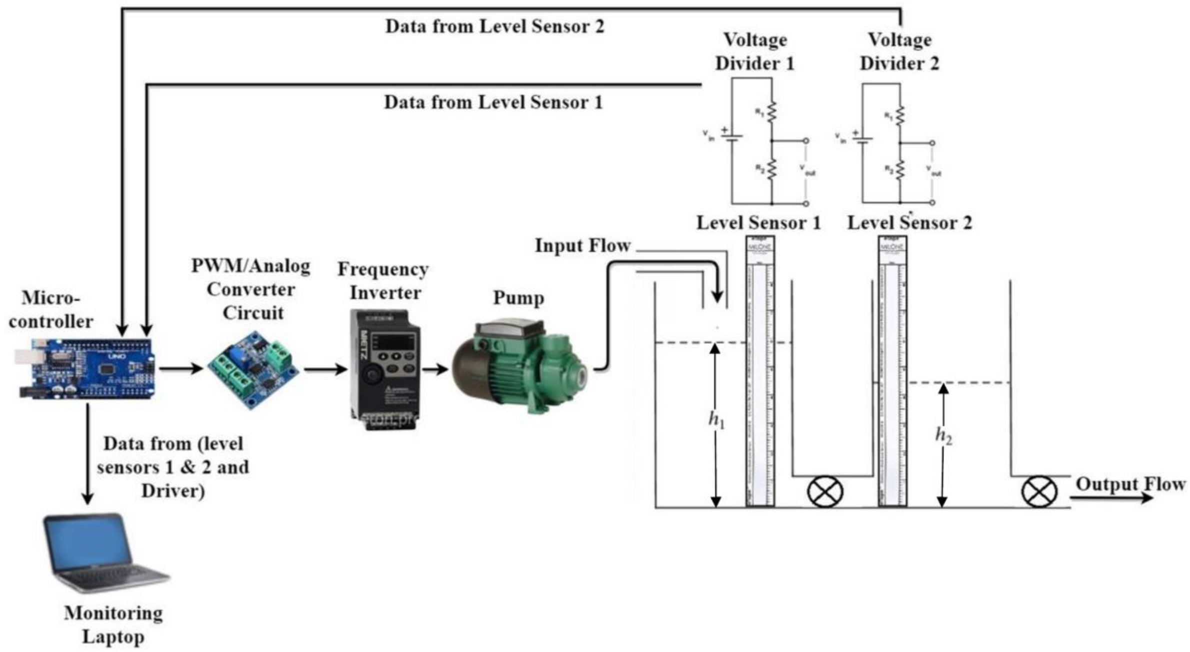

Figure 7. Main components of the horizontal coupled tank system

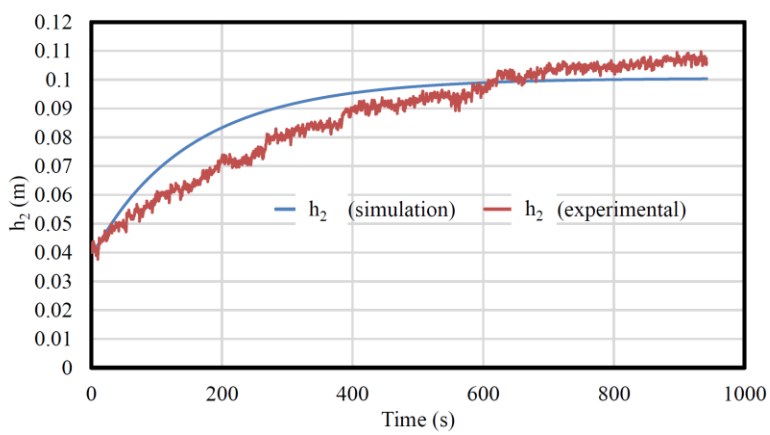

Figure 8. Open-loop test

As shown in Fig. 7, tanks 1 and 2 are connected horizontally via a manually controlled ball valve, which is mounted on the flow channels. The system is configured as follows; the pump discharges water into tank 1, which discharges the water to tank 2 through an intermediate valve to provide dynamic coupling between the two tanks. To minimize the disturbance in the water level and the water splashes inside the tanks from the flowing water, the pipe inside tank 1 from which the water enters the tank, is filled by holes. The height of the liquid level in the two tanks (h_1, h_2) is measured by two level sensors providing the feedback signal to the controller. The outputs from the two-level sensors are connected to the analog inputs of the microcontroller through a voltage divider circuit to convert the sensor resistance change into equivalent voltage.

Depending on the error signal value which is the difference between the measured level and the desired level, the controller sends a control signal (u) in the pulse width modulator (PWM) to the digital output pin of the microcontroller. Consequently, the PWM signal is sent to the PWM/Analog converter circuit to the frequency inverter. The frequency inverter, which is powered by an AC 220V power supply, controls the pump speed, hence controlling the amount of flow flowing into tank 1. The output of the two-level sensors and the control signal (u) are monitored and recorded using an external mode of the microcontroller which is connected to the host computer.

5.2 Open-loop test

In order to verify the derived mathematical model experimentally, an open loop test is implemented such that both the model and the physical system are subjected to a step input flow rate. The experiment is carried out considering all pipelines are filled with water. The level signal is recorded with time for both tests. As can be seen from Fig. 8, there is a little discrepancy between both signals due to model accuracy. However, as will be seen from the controllers' performance curves in the next section, the proposed SMC control algorithms can handle this discrepancy.

5.3 Closed-loop test

In this section, experimental validation of the developed controllers' performances is carried out. The system is given a reference value of 10 cm starting from 4 cm height. The test rig is connected to the host computer through the Arduino Mega 2560 board by using Simulink-MATLAB. First, the PD-SMC model is loaded to the board which operates in external mode for monitoring sensors' readings (h_1, h_2) and the control signal (u). The adopted sample time is 1 second which is found suitable for the system dynamics (closed-loop system time constant ≈ 30 seconds). As can be seen from Fig. 9, the control signal suffered from a high level of fluctuation which affects the performance of the actuator (the frequency inverter and the pump). The actuators' sensitivity to that level of noise hindered the completion of the experimental validation under the effect of sensor noise. Such a high level of chattering could harm the used actuator system.

It is worth noting that all algorithms' controller parameters have been tuned to minimize chattering and error when there is no sensor noise. In order to treat that, a Gaussian-white-noise with SNR (signal-to-noise ratio) with a band of 19-23 dB is superimposed to the sensor in the simulation experiments. Then, in the presence of sensor noise, the optimization method is rerun to obtain the optimum controller parameters., as illustrated in Table 4.

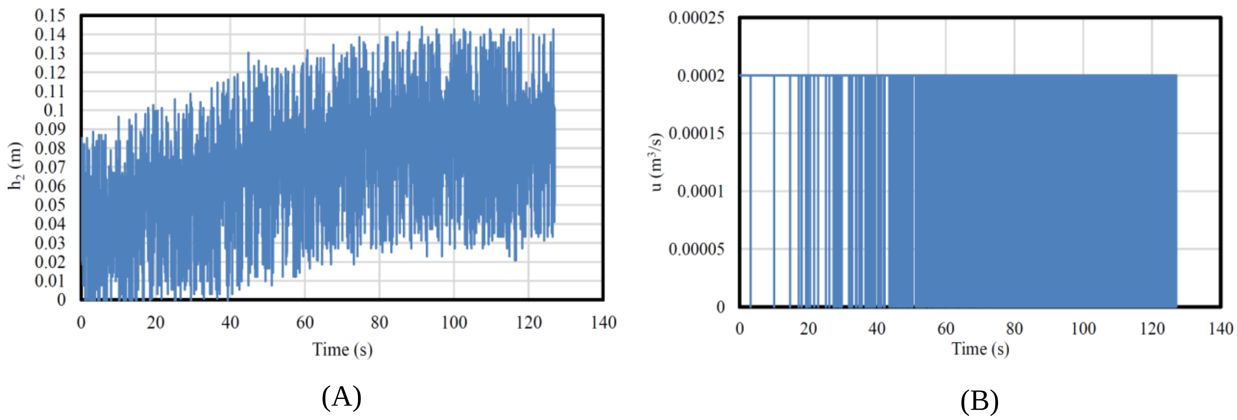

Figure 9. Response of PD-SMC when sensor noise is present: (A) Step response, (B) control

Table 4. New tuning parameters after adding white noise

Parameter \ Algorithm	PD-SMC	PID-SMC	Dynamic-SMC
K	$7.281*10^{6}$	$2.148*10^{12}$	0.146
Δ	$4.366*10^{7}$	$9.600*10^{14}$	2.179
K_p	$3.259*10^{6}$	$6.494*10^{7}$	-
K_I	-	$6.182*10^{6}$	-
K_d	$2.042*10^{7}$	$3.890*10^{8}$	-
α_1	-	-	0.3398
α_2	-	-	0.0493

In order to mitigate sensor noise, a low-pass filter with a cut-off frequency of approximately 1 Hz is added to the controller algorithm. The cut-off frequency is chosen to filter out the sensor noise. Fig. 10 shows the performance of the PD-SMC after adding the designed low-pass filter.

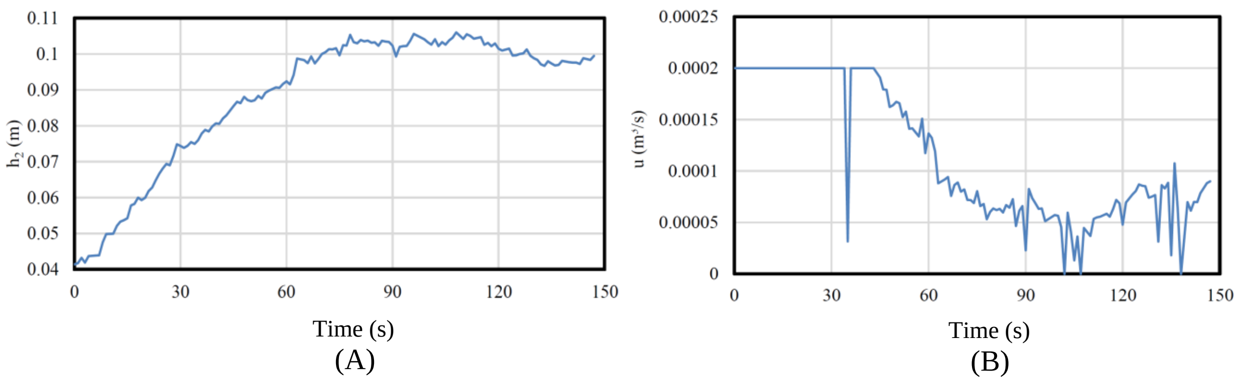

Figure 10. Response of PD-SMC with low-pass filter: (A) 0.1 m step response, (B) Control signal

The same experiment is carried out by using PID-SMC and dynamic-SMC models, see Fig. 11 and Fig. 12. As illustrated in the graphs, PD-SMC showed the minimum value of steady-state error and fluctuation level in the control signal when compared with the other control algorithms, PID-SMC, and dynamic-SMC.

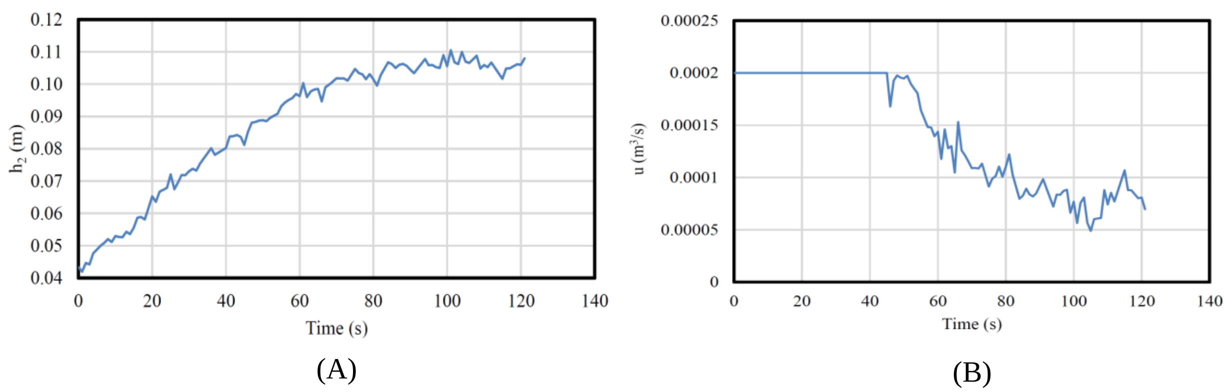

Figure 11. Response of PID-SMC with low-pass filter: (A) Step response, (B) control signal

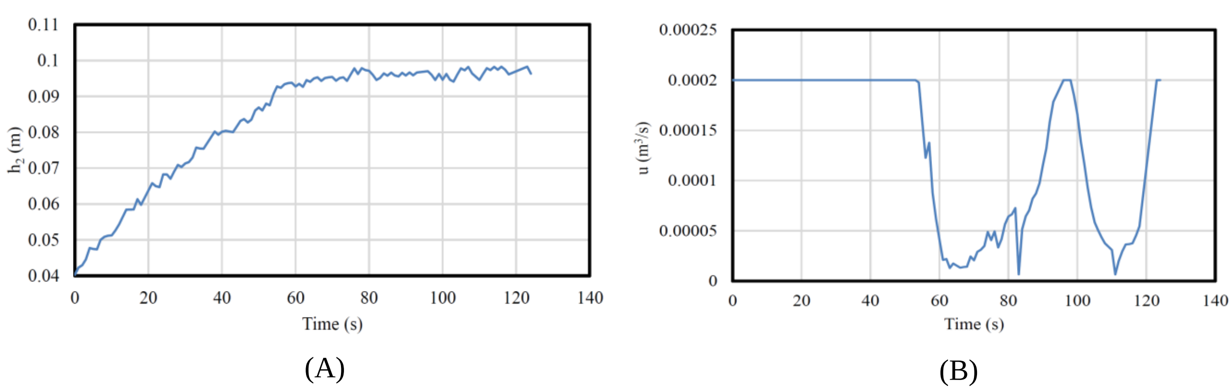

Figure 12. Performance of dynamic-SMC with low-pass filter: (A) 0.1 m step response, (B) control signal

6. Conclusion

In the current paper, the three SMC algorithms' performance for controlling the level of liquid in a horizontally connected tank system is explored. Simulation of the problem facilitates selecting the controller parameter based on optimizing a performance index. The control algorithms are highly sensitive to sensor noise which necessitates filter-out the noises in the band of frequencies of concern. PD-SMC has a superior performance over the other two algorithms, PID-SMC and dynamic-SMC both in simulation and experimental results.

In future work of this research, mathematical analysis of the controller sensitivity to sensor noise level is to be done. Also, a second-dynamic SMC is to be included in the investigation.

- **Acknowledgment**

The authors would like to thank Prof. Dr. Momtaz Sedrak for his valuable advices throughout all stages of this research.

- **Conflict of Interest**

The authors have no conflicts of interest to declare.

7. References

[1] Ko CC, Chen BM, Chen J, Zhuang Y, Tan KC. Development of a web-based laboratory for control experiments on a coupled tank apparatus. IEEE Transactions on education. 2001 Feb;44(1):76-86.

[2] Ang KH, Chong G, Li Y. PID control system analysis, design, and technology. IEEE transactions on control systems technology. 2005 Jun 20;13(4):559-76.

[3] Astrom KJ. PID controllers: theory, design, and tuning. The International Society of Measurement and Control. 1995.

[4] Wang QG, Lee TH, Fung HW, Bi Q, Zhang Y. PID tuning for improved performance. IEEE Transactions on control systems technology. 1999 Jul;7(4):457-65.

[5] Tavakoli S, Griffin I, Fleming PJ. Tuning of decentralised PI (PID) controllers for TITO processes. Control engineering practice. 2006 Sep 1;14(9):1069-80.

[6] Maghade DK, Patre BM. Decentralized PI/PID controllers based on gain and phase margin specifications for TITO processes. ISA transactions. 2012 Jul 1;51(4):550-8.

[7] Wang QG, Zhang Z, Astrom KJ, Zhang Y, Zhang Y. Guaranteed dominant pole placement with PID controllers. IFAC Proceedings Volumes. 2008 Jan 1;41(2):5842-5.

[8] Malwatkar GM, Sonawane SH, Waghmare LM. Tuning PID controllers for higher-order oscillatory systems with improved performance. ISA transactions. 2009 Jul 1;48(3):347-53.

[9] Gaurav AK, Kaur A. Comparison between conventional PID and fuzzy logic controller for liquid flow control: Performance evaluation of fuzzy logic and PID controller by using MATLAB/Simulink. International Journal of Innovative Technology and Exploring Engineering (IJITEE). 2012 Jun;1(1):84-8.

[10] Khalid U, Shah YA, Qamar S, Gohar W, Riaz R, Shah WA. Flow and level control of coupled four tanks system using artificial neural network. American Journal of Computation, Communication and Control. 2014;1(2):30-5.

[11] Cartes D, Wu L. Experimental evaluation of adaptive three-tank level control. ISA transactions. 2005 Apr 1;44(2):283-93.

[12] Pan H, Wong H, Kapila V, de Queiroz MS. Experimental validation of a nonlinear backstepping liquid level controller for a state coupled two tank system. Control Engineering Practice. 2005 Jan 1;13(1):27-40.

[13] Kangwanrat S, Tipsuwannaporn V, Numsomran A. Design of PI controller using MRAC techniques for coupled-Tanks Process. InICCAS 2010 2010 Oct 27 (pp. 485-490). IEEE.

[14] Gouta H, Said SH, Barhoumi N, M'Sahli F. Observer-based backstepping controller for a state-coupled two-tank system. IETE Journal of Research. 2015 May 4;61(3):259-68.

[15] Değirmenci Am, Tan N, Istefanopulos Y. Lag controller design for coupled tank system.

[16] Scheurenberg D, Schmerling K, Abel D. Data Enhanced Model Predictive Control of a Coupled Tank System. In 2022 IEEE/ASME International Conference on Advanced Intelligent Mechatronics (AIM) 2022 Jul 11 (pp. 1646-1651). IEEE.

[17] Aranda-Cetraro I, Pérez-Zúñiga G, Rivas-Pérez R, Sotomayor-Moriano J. Nonlinear Robust Control by a Modulating-Function-Based Backstepping Super-Twisting Controller for a Quadruple Tank System. *Sensors*. 2023; 23(11):5222. https://doi.org/10.3390/s23115222

[18] Mahapatro SR, Subudhi B, Ghosh S. Design and experimental realization of a robust decentralized PI controller for a coupled tank system. ISA transactions. 2019 Jun 1;89:158-68.

[19] Rahman MZU et. al. Fractional Transformation-Based Decentralized Robust Control of a Coupled-Tank System for Industrial Applications. *Fractal and Fractional*. 2023; 7(8):590. https://doi.org/10.3390/fractalfract7080590

[20] Roy P, Roy BK. Fractional order PI control applied to level control in coupled two tank MIMO system with experimental validation. Control Engineering Practice. 2016 Mar 1;48:119-35.

[21] Roy P, Kar B, Roy BK. Fractional order PI-PD control of liquid level in coupled two tank system and its experimental validation. Asian Journal of Control. 2017 Sep;19(5):1699-709.

[22] Kar B, Roy P. A comparative study between cascaded FOPI–FOPD and IOPI–IOPD controllers applied to a level control problem in a coupled tank system. Journal of Control, Automation and Electrical Systems. 2018 Jun;29:340-9.

[23] Prasad GM, Adithya A, Rao AS. Design of multi model fractional controllers for nonlinear systems: an experimental investigation. InComputer Aided Chemical Engineering 2019 Jan 1 (Vol. 46, pp. 1423-1428). Elsevier.

[24] Jegatheesh A, Kumar CA. Novel fuzzy fractional order PID controller for non linear interacting coupled spherical tank system for level process. Microprocessors and Microsystems. 2020 Feb 1;72:102948.

[25] Gurumurthy G, Das DK. An FO-I λ D 1-λ controller design and realization for inverted decoupled Two Input Two Output-Liquid Level System. International Journal of Dynamics and Control. 2020 Sep;8(3):1013-26.

[26] Nath UM, Dey C, Mudi RK. Mathematical modelling and fuzzy knowledge-based decoupled control scheme for real-time interacting level control-MIMO system. International Journal of Modelling and Simulation. 2023 Mar 4;43(2):75-86.

[27] Raj R, Kumar A, Sharma D, Khan S. TS fuzzy controller with s-and z-type MFs to control a coupled-tank system. Materials Today: Proceedings. 2023 Jan 1;80:A8-13.

[28] Slotine JJ, Li W. Applied nonlinear control. Englewood Cliffs, NJ: Prentice hall; 1991 Jan.

[29] Zak SH. Systems and control. New York: Oxford University Press; 2003 Jan.

[30] Utkin V. Variable structure systems with sliding modes. IEEE Transactions on Automatic control. 1977 Apr;22(2):212-22.
[31] Hung JY, Gao W, Hung JC. Variable structure control: A survey. IEEE transactions on industrial electronics. 1993 Feb;40(1):2-2.
[32] Boubakir A, Boudjema F, Boubakir C, Labiod S. A Fuzzy Sliding Mode Controller Using Nonlinear Sliding Surface Applied to the Coupled Tanks System. International Journal of Fuzzy Systems. 2008 Jun 1;10(2).
[33] Mahapatro SR, Subudhi B, Ghosh S. Design and real-time implementation of an adaptive fuzzy sliding mode controller for a coupled tank system. International Journal of Numerical Modelling: Electronic Networks, Devices and Fields. 2019 Jan;32(1):e2485.
[34] Boubakir A, Boudjema F, Labiod S. A neuro-fuzzy-sliding mode controller using nonlinear sliding surface applied to the coupled tanks system. International Journal of Automation and Computing. 2009 Feb;6:72-80.
[35] Aksu IO, Coban R. Sliding mode PI control with backstepping approach for MIMO nonlinear cross-coupled tank systems. International Journal of Robust and Nonlinear Control. 2019 Apr 1;29(6):1854-71.
[36] Almutairi NB, Zribi M. Sliding mode control of coupled tanks. Mechatronics. 2006 Sep 1;16(7):427-41.
[37] Biswas PP, Srivastava R, Ray S, Samanta AN. Sliding mode control of quadruple tank process. Mechatronics. 2009 Jun 1;19(4):548-61.
[38] Khan MK, Spurgeon SK. Robust MIMO water level control in interconnected twin-tanks using second order sliding mode control. Control engineering practice. 2006 Apr 1;14(4):375-86.
[39] Ding S, Park JH, Chen CC. Second-order sliding mode controller design with output constraint. Automatica. 2020 Feb 1;112:108704.
[40] Kashyap R, Jaggi N, Pratap B. Higher-Order Sliding-Mode Observer Based Robust Controller Design for Four-Tank Coupled System. In2019 3rd International conference on Electronics, Communication and Aerospace Technology (ICECA) 2019 Jun 12 (pp. 832-837). IEEE.
[41] Dumlu A, Ayten KK. A combined control approach for industrial process systems using feed-forward and adaptive action based on second order sliding mode controller design. Transactions of the Institute of Measurement and Control. 2019 Feb;41(4):1160-71.
[42] Derdiyok A, Başçi A. The application of chattering-free sliding mode controller in coupled tank liquid-level control system. Korean Journal of Chemical Engineering. 2013 Mar;30:540-5.
[43] Benayache R, Chrifi-Alaoui L, Bussy P, Castelain JM. Design and implementation of sliding mode controller with varying boundary layer for a coupled tanks system. In2009 17th Mediterranean Conference on Control and Automation 2009 Jun 24 (pp. 1215-1220). IEEE.
[44] Delavari H, Ghaderi R, Ranjbar A, Momani S. Fuzzy fractional order sliding mode controller for nonlinear systems. Communications in Nonlinear Science and Numerical Simulation. 2010 Apr 1;15(4):963-78.
[45] Shah DH, Patel DM. Design of sliding mode control for quadruple-tank MIMO process with time delay compensation. Journal of Process Control. 2019 Apr 1;76:46-61.
[46] Calderón AJ, Vinagre BM, Feliu V. Fractional order control strategies for power electronic buck converters. Signal Processing. 2006 Oct 1;86(10):2803-19.
[47] Piazzi A, Visioli A. A noncausal approach for PID control. Journal of Process Control. 2006 Sep 1;16(8):831-43.